Optical studies of bonding in coevaporated amorphous silicon-tin alloys

A. Mohamedi, M. Thèye, M. Vergnat, G. Marchal, M. Piecuch

Optical studies of bonding in coevaporated amorphous silicon-tin alloys

A. Mohamedi and M. L. Thèye
Laboratoire d'Optique des Solides, Université Pierre et Marie Curie, 4 place Jussieu, 75252 Paris CEDEX 05, France

M. Vergnat, G. Marchal, and M. Piecuch
Laboratoire de Physique des Solides, Université de Nancy I, 54506 Vandoeuvre-les-Nancy CEDEX, France
(Received 26 July 1988)

Homogeneous amorphous $Si_{1-x}Sn_x$ alloys have been prepared by coevaporation on cold substrates over a wide composition range, $0 \leq x \leq 0.50$. Their complex dielectric constant $\tilde{\epsilon}$ has been accurately determined between 0.5 and 3 eV by combining different methods on films with different thicknesses (from 30 to 300–500 nm). The derivation of two characteristic alloy parameters (the optical gap and the average gap) from these data is discussed in detail. While the optical gap decreases linearly with increasing x, the average-gap variation shows a change in slope for $x \simeq 0.30$, suggesting a modification of the alloy average bonding. A careful analysis of the overall evolution upon alloying of the ϵ_1 and ϵ_2 spectra supports the conclusion that these a-$Si_{1-x}Sn_x$ alloys are chemically ordered.

I. INTRODUCTION

Although Sn has a very low solid solubility in crystalline Si, amorphous Si-Sn alloys can be obtained as thin films by cosputtering and coevaporation techniques.[1,2] Much attention has recently been paid to hydrogenated a-(Si-Sn) alloys prepared by reactive sputtering,[3–6] glow-discharge decomposition of SiH_4 and SnH_4 mixtures,[7–9] sputter-assisted plasma chemical-vapor deposition[10] and molecular-beam deposition,[11] because of their potentials as low-band-gap materials for multijunction-solar-cell applications. However, in most cases these alloys tend to become inhomogeneous as the Sn concentration increases, because of the segregation of part of the Sn atoms which form crystalline β-Sn precipitates.[2,4,11,12]

Homogeneous a-$Si_{1-x}Sn_x$ alloys, with Sn atoms entering substitutionally the Si network, could be obtained up to Sn atomic concentrations x as high as 0.5 by controlled coevaporation onto substrates maintained at liquid-nitrogen temperature.[2,13] The hydrogenation of these alloys has recently been achieved by introducing atomic hydrogen during evaporation.[14] We present here the results of a detailed study of the optical properties of such coevaporated, nonhydrogenated a-$Si_{1-x}Sn_x$ alloys, with x varying from 0 to 0.5. We determine the changes upon alloying of characteristic parameters like the optical gap and the average gap, and we propose a model for Sn incorporation based on the analysis of the modifications of the complex dielectric constant over a large spectral range.

II. EXPERIMENT

The samples were thin films deposited in an ultrahigh-vacuum chamber (base pressure of the order of 10^{-9} Torr, pressure during deposition lower than 3×10^{-8} Torr), by coevaporation of Si and Sn from an electron-beam gun and a thermal cell, respectively, onto well-polished substrates maintained at liquid-nitrogen temperature. Two calibrated quartz microbalances were used in order to control the evaporation rate of each constituent and to monitor both the composition and the thickness of the films. Deposition rates ranged typically from 0.2 to 0.5 nm/sec.

In order to obtain reliable values of both the real (ϵ_1) and imaginary (ϵ_2) parts of the complex dielectric constant $\tilde{\epsilon}=\epsilon_1+i\epsilon_2=(n+ik)^2$ over a wide spectral range (from 0.5 to 3 eV), we combined the results of different methods applied to films with different thicknesses for a given alloy composition.

In the high-absorption region, we measured both the reflectance (R) and the transmittance (T) at near normal incidence of thin ($\simeq 30$ nm) films, with a Cary-17 spectrophotometer equipped with a V-W specular reflectance attachment. The n and k values were then determined simultaneously from the (R,T) data, using exact thin-film expressions taking into account the coherent multiple reflections in the film and incoherent ones in the transparent substrate.[15] The film thickness needed in the calculations was measured with 1% accuracy by an x-ray interference technique.[16] These thickness values were found to be in excellent agreement (within 1%) for all compositions with those given by the quartz monitoring system, which had been calibrated by multiple-beam interferometry measurements on thicker films (of the order of 200 nm).[13] This indicated that the alloy density did not depend on the film thickness.

In the low-absorption region, in order to improve the accuracy on k (on the absorption coefficient $\alpha=4\pi k/\lambda$), we used thicker films (300–500 nm) and we complemented the traditional transmittance measurements by photothermal deflection spectroscopy (PDS) experiments, performed with the sample immersed in CCl_4, with a 250-W tungsten halogen lamp followed by a H25 Jobin-Yvon monochromator as the exciting source, at a 13-Hz modu-

lation frequency. Since the PDS signal is simply proportional to the film absorptance $A=1-(R+T)$ for thermally thin samples (film thickness much smaller than the thermal diffusion length in the medium), the PDS spectra $S(\hbar\omega)$ were calibrated in all cases by fitting to the true $A(\hbar\omega)$ values computed from the film optical constants as deduced from the transmittance measurements in the usual way, in the region ($\alpha \simeq 10^3-10^4$ cm^{-1}) where the two methods both overlap and give reliable results. The absorption coefficient α was then determined from the calibrated $S(\hbar\omega)$, using appropriate thin-film expressions.[17]

A multilayer analysis of grazing-incidence x-ray reflectometry experiments[18] performed on a few thin alloy films revealed the existence of a superficial contamination layer with a thickness of the order of 3–4 nm.[19] From the value of its x-ray refractive index which can also be deduced from these experiments, it could be inferred that this layer probably consisted in slightly porous or hydrated SiO_2. We checked by model calculations that neglecting the presence of such a contamination layer in the determination of n and k from (R,T) measurements on thin films did not affect the k values but was responsible for a slight decrease of the n values, without noticeable change of the $n(\hbar\omega)$ energy dispersion.

III. ANALYSIS OF THE ALLOY OPTICAL PROPERTIES

A. Complex dielectric constant

Figures 1(a) and 1(b) show the real (ϵ_1) and imaginary (ϵ_2) parts of the complex dielectric constant as a function of energy between 0.5 and 3 eV, determined by the (R,T) method applied to thin films, for a series of a-$Si_{1-x}Sn_x$ alloys with Sn atomic concentration x varying from 0 to 0.59. It must be pointed out that ϵ_1 and ϵ_2 values become slightly less reliable in the (2.5–3)-eV range, because of larger uncertainties due to problems inherent in the search of (n,k) solutions by the (R,T) method,[20] and that the accuracy on the ϵ_2 values in the low-absorption (low-energy) range is rather poor since very thin films have been used in these experiments. Two remarks can be made about these spectra.

While for the alloys with $x \leq 0.50$ the overall shape of the ϵ_1 and ϵ_2 spectra remain roughly similar to that for pure a-Si, with only minor modifications to be studied later, it changes drastically for the two alloys with $x > 0.50$. This reflects the fact that these samples are no longer homogeneous, since they contain metallic β-Sn crystallites embedded in the amorphous semiconducting matrix, as shown by electron microscopy and electron diffraction studies.[2] In the following, we will only consider the homogeneous $a-Si_{1-x}Sn_x$ alloys, with x varying from 0 to 0.50.

The general trends observed upon alloying are, as expected, a shift of the ϵ_2 spectrum to lower energies and an increase of the sub-band-gap ϵ_1 values. However, it appears very clearly, when looking for example at the shape of the ϵ_2 edge and at the location of the broad maximum in the ϵ_1 spectrum, that the alloys can be separated into two groups: Si-rich alloys, for $x \leq 0.195$, which exhibit a Si-like optical behavior and Sn-rich alloys, for $0.31 \leq x \leq 0.495$. This is a first indication of a possible change in average bonding for Sn concentrations between 0.2 and 0.3.

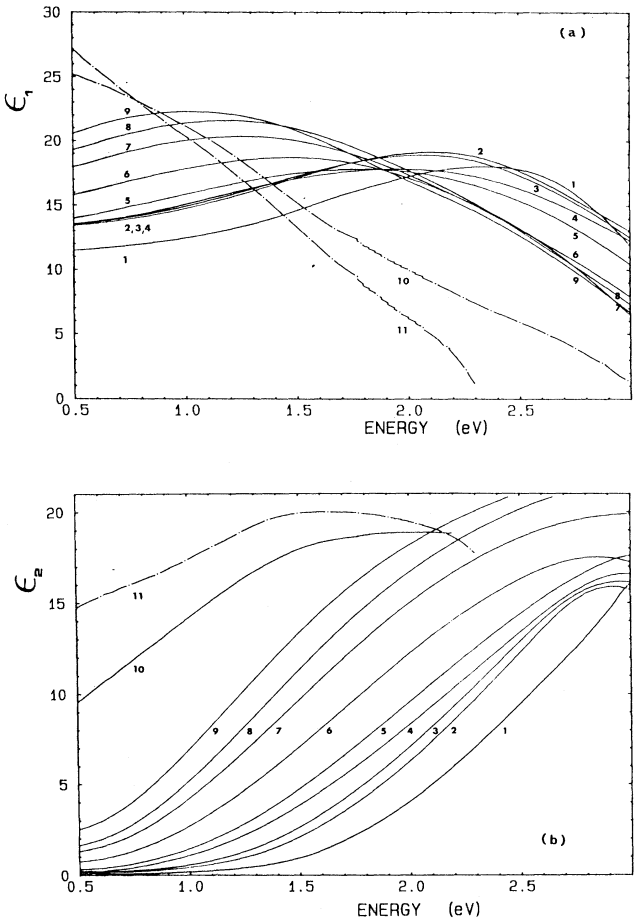

FIG. 1. (a) Real (ϵ_1) and (b) imaginary (ϵ_2) parts of the complex dielectric constant vs energy for a-$Si_{1-x}Sn_x$ alloys with Sn atomic concentrations (1) $x=0$, (2) 0.055, (3) 0.095, (4) 0.15, (5) 0.195, (6) 0.31, (7) 0.38, (8) 0.42, (9) 0.495, (10) 0.55, (11) 0.59.

B. Optical gap

In the region of the absorption edge where the absorption coefficient α is high enough ($\alpha \gtrsim 10^4$ cm^{-1}) that the corresponding optical absorption can without any doubt be assigned to electronic transitions between extended states in both the valence and conduction bands, it has been proposed[21] that the imaginary part of the complex dielectric constant behaves as

$$(\hbar\omega)^2\epsilon_2 = B^2(\hbar\omega - E_0)^2 . \quad (1)$$

This relation has been derived from the general one-electron ϵ_2 expression,

$$\epsilon_2(\hbar\omega)=\left[\frac{2\pi e\hbar}{m}\right]^2\frac{1}{(\hbar\omega)^2}\frac{2}{V}\sum_{v,c}|P_{v,c}|^2\,\delta(E_v-E_c-\hbar\omega)\ , \tag{2}$$

where E_v and E_c are the energies of the initial and final states of the optical transitions and $P_{v,c}=\langle c|P|v\rangle$ is the corresponding momentum matrix element. When applying the "nondirect"-transition model in which only the energy is conserved in the transitions, expression (2) then becomes

$$\epsilon_2(\hbar\omega)\sim\frac{1}{(\hbar\omega)^2}P^2(\hbar\omega)\int g_v(E)g_c(E+\hbar\omega)dE\ , \tag{3}$$

where $g_v(E)$ and $g_c(E)$ are the valence- and conduction-band densities of states, and P^2 is the average momentum matrix element squared. Relation (1) is obtained from expression (3) under the assumptions of a square-root energy dependence of the densities of states at the band edges, and of constant average momentum matrix element. The optical gap E_0 determined by extrapolation from relation (1) thus represents some measure of the energy separation between extended states in the valence and conduction bands, and is commonly considered as a useful parameter for characterizing amorphous semiconductors, even if its physical meaning remains unclear. It may be added that recent theoretical calculations[22] have confirmed the general validity of relation (1), even though the assumptions involved in the original Tauc model may be questionable.

Figure 2 shows plots of the quantity $\hbar\omega(\epsilon_2)^{1/2}$ versus energy between 0.5 and 3 eV for pure a-Si and for the series of a-$Si_{1-x}Sn_x$ alloys with x varying from 0.055 to 0.495. As emphasized earlier, the use of thin films for the optical measurements allowed us to determine ϵ_2 over a large absorption range. It can immediately be seen in Fig. 2 that, if relation (1) is followed very well for Sn-rich alloys with $x\geq 0.31$, over a wide spectral range (1 eV and more), leading to an unambiguous determination of the optical gap E_0, this is not the case for pure a-Si and, to a lesser extent, for Si-rich alloys with ≤ 0.19. Especially for pure a-Si, the curvature is so important that no reliable E_0 value can be obtained; depending on the edge region chosen for the extrapolation, E_0 can vary by more than 0.2 eV.

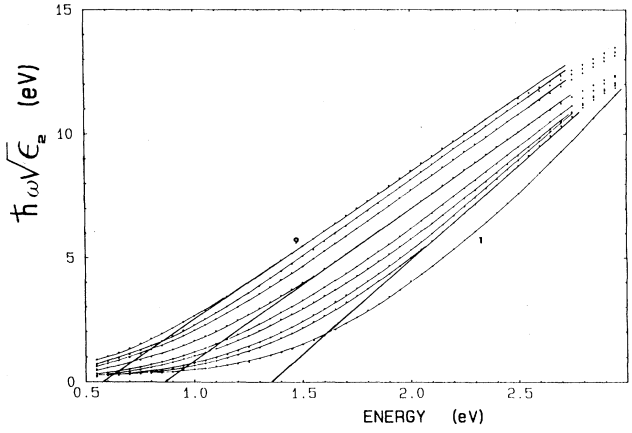

FIG. 2. Plots of the quantity $\hbar\omega(\epsilon_2)^{1/2}$ vs energy according to the Tauc model for the same a-$Si_{1-x}Sn_x$ alloys as in Fig. 1, with x varying from 0 to 0.495; the straight lines used for the optical gap determination are drawn in a few cases only.

While relation (1) was found to be well obeyed for many amorphous tetrahedrally bonded semiconductors,[23,24] deviations have already been reported and discussed for hydrogenated a-Si, and different laws which better reproduce the optical data have been proposed.[25,26] These laws are justified by a modification of the assumptions made in the original Tauc model: either by changing the energy dependence of the densities of states at the band edges,[25] or by arguing that the average dipole matrix element, instead of the average momentum matrix element, must be taken as a constant (independent of energy).[26] This last assumption is indeed consistent with the results of matrix-element calculations performed for the so-called ST-12 crystalline polytype of Si, which presents structural analogies with amorphous Si,[27] as well as with the results of an experimental determination of the energy dependence of the matrix element from a combination of complex dielectric constant and density-of-states measurements on a-Si:H.[28] Since expression (2) can also be written[28]

$$\epsilon_2(\hbar\omega)=(2\pi e)^2\frac{2}{V}\sum_{v,c}|R_{v,c}|^2\,\delta(E_c-E_v-\hbar\omega)\ , \tag{4}$$

where $R_{v,c}=\langle c|r|v\rangle$ is now the dipole matrix element, the nondirect-transition model leads to

$$\epsilon_2(\hbar\omega)\sim R^2(\hbar\omega)\int g_v(E)g_c(E+\hbar\omega)dE \tag{5}$$

and, under the assumptions of constant average dipole matrix element and parabolic band edges, one obtains

$$\epsilon_2(\hbar\omega)=(B')^2(\hbar\omega-E_0')^2\ . \tag{6}$$

This relation, which replaces Eq. (1) for the determination of the optical gap, was found to be well followed for a-Si:H,[26,29] with an E_0' value appreciably lower than the E_0 values which could be deduced when applying relation (1) to the same data. Figure 3 shows that our ϵ_2 values for pure a-Si are indeed rather well reproduced by relation (6) over about 1 eV. The corresponding E_0' value, of the order of 1.05 eV, is, however, very small compared to the E_0 values which can reasonably be deduced from the plots of Fig. 2 (between 1.3 and 1.7 eV). On the other hand, relation (6) does not seem to apply to the a-$Si_{1-x}Sn_x$ alloys, especially the Sn-rich alloys, for which it leads to unphysical results (negative value for the optical gap). This discussion demonstrates that the problem of the optical absorption due to transitions between extended states close to the band edges is far from being solved, since no unique model is able to correctly reproduce the optical data in the a-$Si_{1-x}Sn_x$ system for all x values from 0 to 0.5. This means that one should take properly into account in each case the exact energy dependence of both the band-edge densities of states and the optical matrix element. Since, however, the Tauc model seems to give better results for the alloy series, we

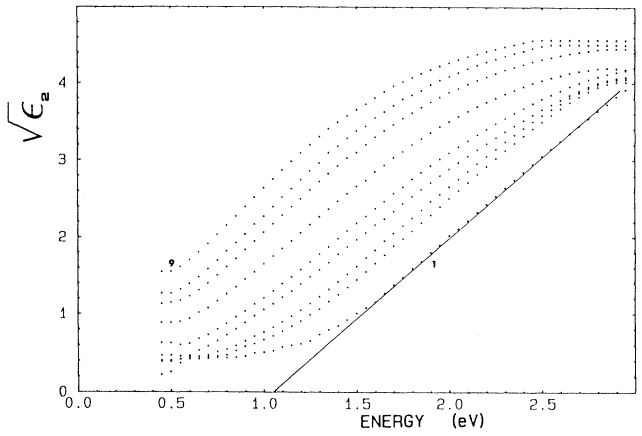

FIG. 3. Plots of the quantity $(\epsilon_2)^{1/2}$ vs energy for the same a-$Si_{1-x}Sn_x$ alloys as in Fig. 3; the straight line used for the optical gap determination is drawn in the pure a-Si case only.

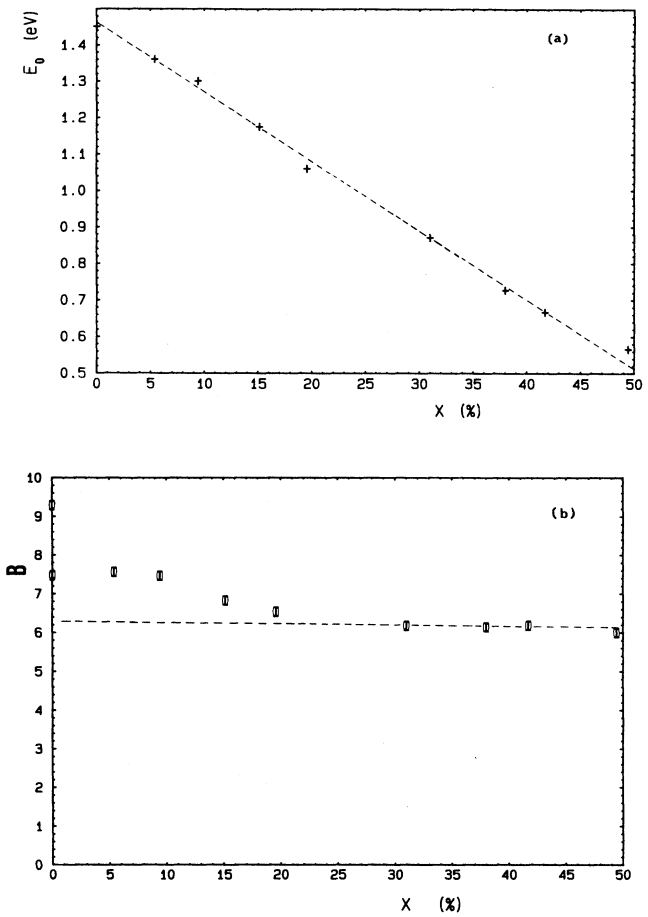

FIG. 4. Variation with the Sn atomic concentration x of (a) the optical gap E_0 and (b) of the "slope" of the edge B as deduced from the Tauc model for a-$Si_{1-x}Sn_x$ alloys.

will use this model in the following.

The variations of the two characteristic parameters, the optical gap E_0 and the "slope" of the edge B, versus Sn concentration x between 0.055 and 0.495, are reported in Fig. 4(a) and 4(b), respectively. These values have been determined by considering systematically the high-energy (high-absorption) part of the plots of Fig. 2. Under such conditions, the optical gap E_0 decreases linearly with increasing x over the whole composition range, according to $E_0 = 1.45 - 1.87x$ eV. One can notice that the E_0 value for $x = 0$, 1.45 eV, corresponds to the value which would be deduced for pure a-Si by extrapolation of the intermediate, and not upper, part of the edge. A zero-gap value would be obtained for an alloy with $x = 0.775$. The present decrease of E_0 upon alloying is slightly slower than the ones reported previously for coevaporated or sputtered nonhydrogenated alloys.[1,30] This probably comes from the fact that the optical measurements were then performed on thicker films (i.e., over a smaller spectral range) and over a more narrow x range, and that their analysis ignored the effects discussed above. Contrary to E_0, the slope B does not show a smooth variation with x. It first decreases with increasing x up to $x = 0.19$ and then remains approximately constant. This behavior simply reflects the changes in the shape of the absorption edge when incorporating Sn to a-Si. One can notice that, for Sn-rich alloys with $x \geq 0.31$, for which the Tauc model applies very well, the edge shifts parallel to itself towards low energies with increasing x.

C. Average gap

The real part ϵ_1 of the complex dielectric constant at energies smaller than the optical gap can be related to some "average" gap which, contrary to the optical gap, does not represent a real (pseudo) gap in the density of states, but can rather be considered as a measure of the average energy separation between valence and conduction states, representative of the average bonding strength in the material. Various models have been proposed in order to derive such an average gap. We first consider the single "effective oscillator" description of the frequency dependence of the refractive index n in the sub-band-gap region:[32–34]

$$n^2(\hbar\omega) = 1 + \frac{E_d E_W}{E_W^2 - (\hbar\omega)^2} \quad . \tag{7}$$

E_W is the energy of the effective oscillator and E_d is a so-called "dispersion energy," which is claimed to measure the average strength of the optical interband transitions and to depend essentially on the ionicity, the chemical valency, and the coordination number, and not on the volume density of the valence electrons. For pure a-Si and for Si-rich alloys up to $x = 0.19$, the experimental energy dispersion of n is well reproduced by relation (7) over a rather large spectral range, as shown in Fig. 5, and the two parameters E_W and E_d can be accurately determined. For higher Sn concentrations, because of the sudden shift to lower energies of the broad maximum of the n or ϵ_1 spectrum [see Fig. 1(a)], the available energy range becomes very small and, although relation (7) can still be

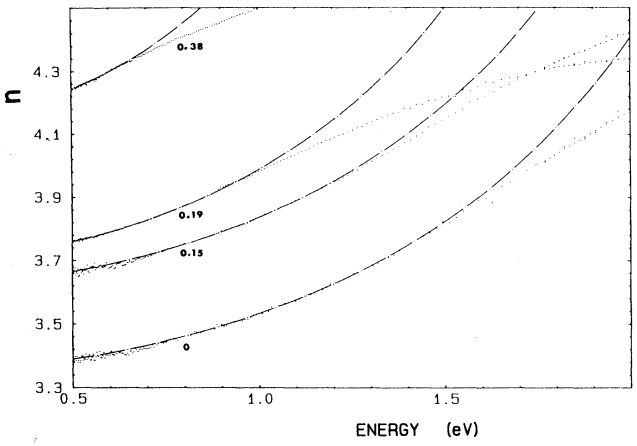

FIG. 5. Examples of fits of the energy dispersion of the real part n of the index of refraction with the "effective oscillator" expression (7) for pure a-Si and for three a-$Si_{1-x}Sn_x$ alloys; the dots represent the experimental n values, the dashed-dotted curves the results of the fits.

applied, the E_W and E_d determination is less reliable. The variations of these two parameters with x over the whole composition range are, nevertheless, reported in Fig. 6. It must be pointed out that E_W, which depends essentially on the n energy dispersion, is practically not affected by the errors due to the presence of a contamination layer on the samples, but that E_d, which depends on the n absolute values, must be slightly underestimated (by a few percent). E_W, which is of the order of 3 eV for pure a-Si, in agreement with a previous estimate,[34] decreases linearly with increasing x for $x \leq 0.19$. For higher Sn concentrations, E_W starts to decrease more rapidly. This coincides with a general change in the alloy optical behavior, as pointed out before. As for E_d, it remains practically constant over the whole composition range and equal to about 33 eV, a value again in agreement with a previous estimate for a-Si.[34] The fact that E_d does not change upon alloying is consistent with the prediction of the model, since the substitutional incorporation of Sn atoms into the a-Si network does not modify its average coordination. This expected behavior of the experimental E_d values gives confidence that the experimental E_W values obtained simultaneously are reliable over the whole composition range.

We now use the spectroscopic theory of bonding,[35,36] based on the simple isotropic free-electron model containing a single energy gap E_g proposed by Penn.[37] In this model, the static (real) dielectric constant $\epsilon(0)$ can be expressed as

$$\epsilon(0)=n^2(0)=1+A\frac{(\hbar\omega_p)^2}{E_g^2} . \tag{8}$$

E_g is an average gap representing the average energy separation between bonding and antibonding states, $\hbar\omega_p=(4\pi Ne^2/m)^{1/2}$ is the plasma energy associated with the four valence electrons (N being their number per unit volume, e the charge, and m the mass of the free electron) and A accounts for matrix-element effects. One can notice that if the two average gaps E_W and E_g are assumed to be equal, expression (7) reduces to expression (8) for $\hbar\omega=0$, provided $E_W E_d = A(\hbar\omega_p)^2$. We have determined E_g from the $n(0)$ values obtained by extrapolation of the experimental data with expression (7), using for $\hbar\omega_p$ the values calculated with the alloy densities as measured in a previous work,[2] and taking $A=1$. These E_g values are reported as a function of x in Fig. 7, together with the E_W values obtained with the other model. It must be recalled that E_g, which depends on the n absolute values, may be slightly affected by the errors due to the contamination layer. The unexpectedly high value for pure a-Si might be due to the presence of a thicker superficial layer and/or to a more important porosity. Figure 7 shows that although the E_g values are larger than the E_W values, they follow the same trends upon alloying. They first decrease linearly with increasing x (for $x \leq 0.19$), at about the same rate as the E_W values, and then their variation becomes more rapid. It is interesting to notice that E_g would be equal to E_W if A was taken to be of the order of 0.63, a value which is close to $A=\frac{2}{3}$ estimated in the Penn model.[38]

It has been proposed[35] that the average gap E_g should

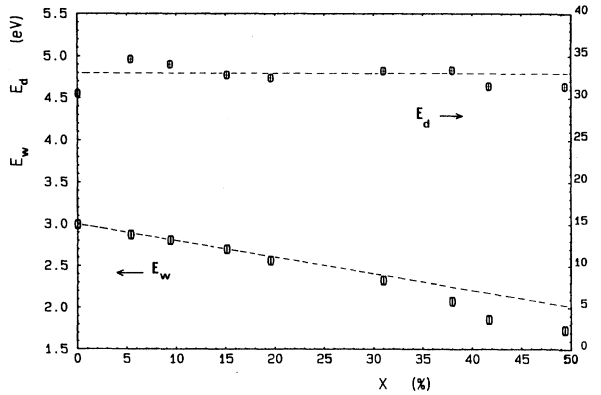

FIG. 6. Variation with the Sn atomic concentration x of the average gap E_W and of the dispersion energy E_d as deduced from the "effective oscillator" model for a-$Si_{1-x}Sn_x$ alloys.

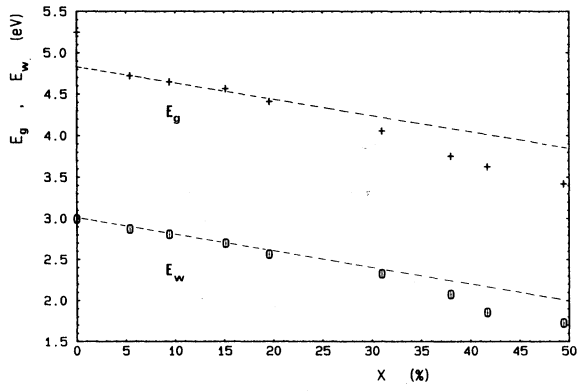

FIG. 7. Variation with the Sn atomic concentration x of the Wemple average gap E_W and of the Penn average gap E_g for a-$Si_{1-x}Sn_x$ alloys.

vary with the average interatomic distance d according to $E_g^2 \sim d^{-5}$. This prediction was indeed verified in the case of sputtered a-$Ge_{1-x}Sn_x$ alloys, with $x=0$, 0.25, and 0.50, which were known to present a random nearest-neighbor environment.[39] In the case of the present a-$Si_{1-x}Sn_x$ alloys, using the d values determined in a previous study,[13] we found that the $E_g^2 d^5$ product remained constant within 2% for the Si-rich alloys up to $x=0.19$. For higher Sn contents, this quantity started to decrease regularly with increasing x. This again suggested a change in the average bonding for x between 0.2 and 0.3.

One can wonder whether there is a correlation between the variations upon alloying of the average gap, which represents the average energy separation between the valence- and conduction-band states considered as a whole, and the optical gap, which corresponds to the distance between the band edges. Figure 8 shows the E_W values plotted as a function of the E_0 values over the entire composition range. For the Sn-rich alloys ($x \geq 0.31$), E_W decreases linearly with E_0, with a slope nearly to 1, indicating that the width of the (pseudo) gap follows the bonding-antibonding splitting, as expected from a simple tight-binding model. For the Si-rich alloys ($x \leq 0.19$), E_W decreases less rapidly than E_0. This different behavior suggests that, at low Sn concentrations, alloying affects more strongly the location (and probably the shape) of the band edges than the bulk of the bands which determines the average bonding strength.

D. Absorption edge

Figure 9 shows the optical-absorption coefficient α as a function of energy between 1.5 and 0.5 eV for pure a-Si and for a series of a-$Si_{1-x}Sn_x$ alloys with x ranging from 0.10 to 0.49. As explained before, these data have been obtained from a combination of optical and photothermal deflection measurements on thick films. α decreases smoothly with decreasing energy for all samples, and no structure can be detected on these spectra. This means that, contrary to the case of a-Si:H,[40] it is impossible to separate out the contributions of optical transitions in-

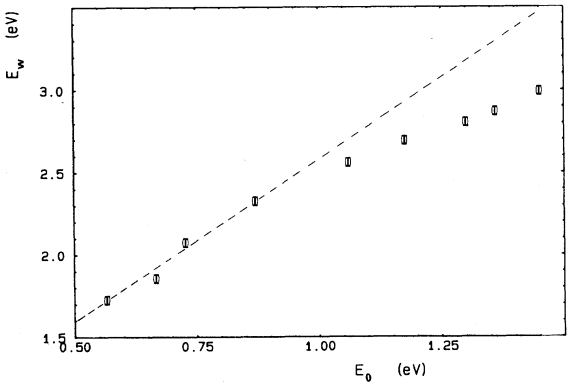

FIG. 8. Average gap E_W vs optical gap E_0 for a-$Si_{1-x}Sn_x$ alloys with x varying from 0 to 0.495.

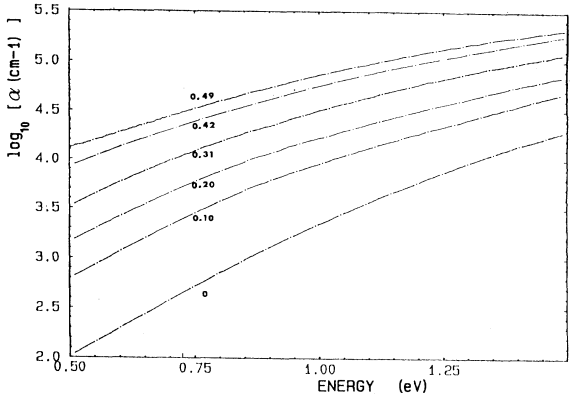

FIG. 9. Logarithm of the optical-absorption coefficient $\alpha=4\pi k/\lambda$ vs energy in the edge region for a-$Si_{1-x}Sn_x$ alloys with x varying from 0 to 0.49.

volving, respectively, disorder-induced band-tail states, and defect states located deeper in the gap. Such a result was to be expected for films deposited at liquid-nitrogen temperature which, even after annealing at room temperature, must be very disordered and contain a high proportion of defects of various kinds (dangling bonds, weak bonds, etc.) The tail states and defect states must at least partially overlap and the total density of localized states throughout the pseudogap must be very high, especially for the low-band-gap Sn-rich alloys. This was indeed confirmed by dc-conductivity measurements performed on identically prepared alloy films, analyzed in terms of variable-range hopping in localized states at the Fermi level.[41] The density of states at the Fermi level was found to increase from 8×10^{19} eV^{-1} cm^{-3} for $x=0.10$ to 1.6×10^{21} $eV^{-1}cm^{-3}$ for $x=0.48$.

IV. DISCUSSION

Controlled coevaporation onto substrates maintained at low temperature has allowed to obtain homogeneous amorphous $Si_{1-x}Sn_x$ alloy films, with Sn atoms entering the tetracoordinated a-Si network substitutionally, for x between 0 and 0.5. It was thus possible to investigate the effects of alloying in this IV-IV amorphous system over a wide composition range. The optical gap E_0, determined by extrapolation of the high-absorption part of the ϵ_2 edge according to the Tauc model, was found to decrease linearly with increasing x over the whole composition range, except for $x=0$ where the Tauc model did not apply. On the contrary, the variation of the average gap as deduced, either from the $n(\hbar\omega)$ variation, E_W, or from the $n(0)$ values, E_g, exhibited a change in slope for x of the order of 0.2–0.3, which pointed to some modification of the alloy average bonding strength for such Sn concentrations. A closer examination of both the ϵ_1 and ϵ_2 spectra determined over a large spectral range (from 0.5 to 3 eV) shows that these spectra do not evolve smoothly upon alloying. While for $x \leq 0.19$ their behavior remains essentially Si-like, more drastic changes are observed for

$x \geq 0.31$ and the evolution of both ϵ_1 and ϵ_2 becomes more rapid. If we refer to the predictions of the tetrahedron-based model proposed for the optical response of such IV-IV alloys[42] along the lines of previous works,[43,44] this indicates that our a-$Si_{1-x}Sn_x$ alloys are not chemically disordered.

The presence of chemical ordering was already suggested by the results of previous experiments performed on identically prepared a-$Si_{1-x}Sn_x$ alloys.[13] The most convincing evidence comes from Mössbauer experiments, which showed that each Sn atom tends to be selectively surrounded by four Si atoms. An additional argument is provided by a comparison between the experimental interference functions deduced from electron diffraction experiments and the ones computed for two continuous random network models with different topologies,[45,46] which suggests that, as the Sn content increases, the alloy structure is better and better described by the model containing even-membered rings only, more compatible with chemical ordering.[47]

We therefore assume that our a-$Si_{1-x}Sn_x$ alloys are chemically ordered, which means that they contain the maximum possible number of "heteropolar" Si—Sn bonds and that, in the investigated composition range (Si-rich side), Sn atoms have only Si nearest neighbors. The observed evolution upon alloying of the complex dielectric constant can then be qualitatively analyzed in relation with the variations of the Si- and Sn-centered tetrahedra probabilities.[42] At low Sn concentrations, Si-centered tetrahedra, especially Si-Si_4 ones, are predominant, which explains the Si-like behavior of the optical properties. As the Sn content increases, the influence of Sn-Si_4 tetrahedra becomes more and more important and is responsible for more pronounced changes in the dielectric constant. It is worth noticing, however, that since the alloys under study are probably not completely chemically ordered, the presence of some Sn—Sn bonds, which are expected to absorb at very low energies, may also contribute significantly to the observed $\tilde{\epsilon}$ modifications, even if present in low concentrations.

In order to verify this assumption, we propose a simple model which consists in regarding the a-$Si_{1-x}Sn_x$ alloys as mixtures, on a microscopic scale, of two components: a-Si and a-$Si_{0.5}Sn_{0.5}$, according to the formula a-$(Si_{0.5}Sn_{0.5})_{1-\delta}Si_\delta$; $\delta = 1-2x$ represents the excess of Si with respect to the stoichiometric composition of the Si-Sn "compound." The effective complex dielectric constant $\bar{\epsilon}$ of such an inhomogeneous medium can be determined via the Bruggemann effective-medium approximation (EMA),[48] which gives

$$q\frac{\epsilon_a-\bar{\epsilon}}{\epsilon_a+2\bar{\epsilon}}+(1-q)\frac{\epsilon_b-\bar{\epsilon}}{\epsilon_b+2\bar{\epsilon}}=0\ . \tag{9}$$

ϵ_a and ϵ_b are, respectively, the complex dielectric constant of pure a-Si and of a-$Si_{0.5}Sn_{0.5}$, as determined in the present work, while q and $1-q$ are their volumic fractions, computed for each Sn atomic concentration, using the appropriate tetahedron volumes obtained with the density values measured for $x=0$ and 0.5. The results of these computations for x values corresponding to the investigated alloys are shown in Figs. 10(a) and 10(b). The calculated spectra reproduce the main trends of the experimental spectra [Figs. 1(a) and 1(b)] upon alloying, namely a change in the shape of the ϵ_2 edge and a sudden shift of the broad ϵ_1 maximum towards low energies for $x > 0.19$. This overall agreement supports our assumption that a-$Si_{1-x}Sn_x$ alloys are chemically ordered. The slight discrepancies which are observed between the two sets of results might be explained by uncertainties on the experimental data. They could also indicate that a more sophisticated model, properly taking into account the optical response of all possible Si- and Sn-centered tetrahedra,[42,44] would be more appropriate than the simple model used here.

One may notice that, for a tetrahedrally coordinated AB network which is perfectly chemically ordered and homogeneous with respect to the spatial distribution of A—B bonds, the "percolation threshold," i.e., the B concentration beyond which an infinite self-avoiding walk on the A subnetwork is no longer possible, is equal to 0.33.[49] This percolation threshold corresponds roughly to the Sn

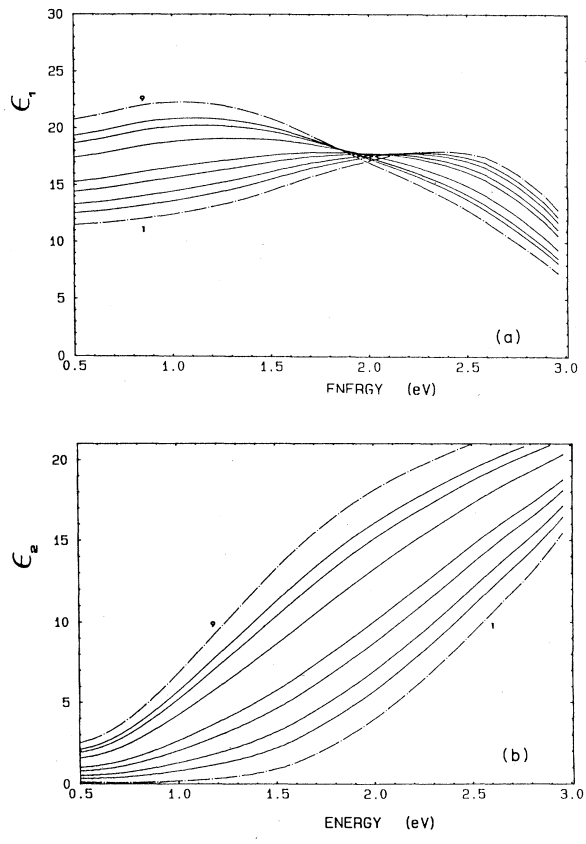

FIG. 10. Real (ϵ_1) and (b) imaginary (ϵ_2) parts of the complex dielectric constant vs energy, as computed with the effective-medium approximation for a-$(Si_{0.5}Sn_{0.5})_{1-\delta}Si_\delta$ mixtures corresponding to the a-$Si_{1-x}Sn_x$ alloys of Fig. 1, with x varying from 0 to 0.495.

concentration at which the a-$Si_{1-x}Sn_x$ alloy optical properties change from a Si-like to a Si-Sn-like behavior, but seems to be slightly higher; the alloy with $x=0.31$ is indeed already Si-Sn-like. This discrepancy might indicate that the tetrahedra, rather than the bonds, are the proper structural units determining the optical response of the alloys, as already suggested.[42–44]

It is worth pointing out in the end that our conclusions about the nature of bonding in coevaporated a-$Si_{1-x}Sn_x$ alloys is opposite that deduced from careful structural and optical studies on cosputtered a-$Ge_{1-x}Sn_x$ alloys, which were found to have a random nearest-neighbor environment.[39] The preferential occurrence of "heteropolar" Si—Sn bonds in a-$Si_{1-x}Sn_x$ alloys can first be explained by the large size difference between the atoms of the two constituents (0.235 nm for Si, compared to 0.280 nm for Sn), which favors local configurations in which a Sn atom is rather surrounded by Si atoms than by Sn atoms. However, since Si has a somewhat higher electronegativity than Sn, chemical effects cannot completely be discarded. Photoemission and x-ray spectroscopy studies of the electronic state distributions are under way in order to bring additional information on this problem.[50] It would also be interesting to perform extended x-ray-absorption fine-structure spectroscopy studies of the local environment around both Si and Sn atoms as a function of the alloy composition, in order to obtain a more direct confirmation of the presence of chemical ordering.

ACKNOWLEDGMENTS

The Laboratoire d'Optique des Solides (Université Pierre et Marie Curie) is "Unité Associée du Centre National de la Recherche Scientifique (CNRS) No. 781"; the Laboratoire de Physique des Solides (Université de Nancy I) is "Unité Associée du CNRS No. 155."

[1]C. Verie, J. F. Rochette, and J. P. Rebouillat, J. Phys. (Paris) Colloq. **42**, C4-667 (1981).
[2]M. Vergnat, G. Marchal, M. Piechuch, and M. Gerl, Solid State Commun. **50**, 237 (1984).
[3]D. L. Williamson, J. Appl. Phys. **55**, 2816 (1984).
[4]G. Chen, F. Zhang, N. Zhang, and D. He, Solar Energy Mater. **12**, 471 (1985).
[5]A. Morimoto, T. Kataoka, and T. Shimizu, Jpn. J. Appl. Phys. **24**, 1122 (1985).
[6]G. N. Parsons, J. W. Cook, G. Lucovsky, S. Y. Lin, and M. J. Mantini, J. Vac. Sci. Technol. A **4**, 470 (1986).
[7]A. H. Mahan, D. L. Williamson, and A. Madan, Appl. Phys. Lett. **44**, 220 (1984).
[8]B. Von Roedern, A. H. Mahan, R. Konenkamp, D. L. Williamson, A. Sanchez, and A. Mahan, J. Non-Cryst. Solids **66**, 13 (1984).
[9]W. Xu, Y. Yin, and C. Lee, J. Non-Cryst. Solids **77-78**, 905 (1985).
[10]H. Itozaki, N. Fujita, T. Igarashi, and H. Hitotsuyanagi, J. Non-Cryst. Solids **59-60**, 589 (1983).
[11]D. Girginoudi, A. Thanailakis, and A. Christou, in *Interfaces, Superlattices and Thin Films,* Vol. 77 of *The Materials Research Society Symposium Proceedings,* edited by J. D. Dow and I. K. Schuller (MRS, Pittsburgh, 1987), p. 603.
[12]K. M. Jones, D. L. Williamson, and B. G. Yacobi, J. Appl. Phys. **56**, 1220 (1984).
[13]M. Vergnat, M. Piecuch, G. Marchal, and M. Gerl, Philos. Mag. B **51**, 327 (1985).
[14]M. Vergnat, G. Marchal, and M. Piecuch, Rev. Phys. Appl. **22**, 1803 (1987).
[15]F. Abeles and M. L. Theye, Surf. Sci. **5**, 325 (1966).
[16]H. Kiessig, Ann. Phys. (Leipzig) 10, 769 (1931); W. Umrath, Z. Angew. Phys. **22**, 406 (1967).
[17]K. Driss-Khodja, A. Gheorghiu, and M. L. Theye, Opt. Commun. **55**, 169 (1985).
[18]P. Croce, L. Nevot, and B. Pardo, Nouv. Rev. Opt. Appl. **3**, 37 (1972).
[19]L. Nevot, B. Pardo, and J. Corno (private communication).
[20]P. O. Nilsson, Appl. Opt. **7**, 435 (1968).
[21]J. Tauc, R. Grigorovici, and A. Vancu, Phys. Status Solidi **15**, 627 (1966); J. Tauc, in *Amorphous and Liquid Semiconductors,* edited by J. Tauc (Plenum, London, 1974), Chap. 4.
[22]S. Abe and G. Toyozawa, J. Phys. Soc. Jpn. **50**, 2185 (1981).
[23]M. L. Theye, in *Optical Properties of Solids: New Developments,* edited by B. O. Seraphin (North-Holland, Amsterdam, 1976), p. 353.
[24]A. Gheorghiu and M. L. Theye, Philos. Mag. B **44**, 285 (1981).
[25]R. H. Klazes, M. H. L. M. Van Den Broek, J. Bezemer, and S. Radelaar, Philos. Mag. B **45**, 377 (1982).
[26]G. D. Cody, B. G. Brooks, and B. Abeles, Solar Energy Mater. **8**, 231 (1982).
[27]J. D. Joannopoulos and M. L. Cohen, Phys. Rev. B **8**, 2733 (1973).
[28]W. B. Jackson, S. M. Kelso, C. C. Tsai, J. W. Allen, and S. J. Oh, Phys. Rev. B **31**, 5187 (1985).
[29]G. D. Cody, in *Semiconductors and Semimetals,* edited by J. I. Pankove (Academic, Orlando, 1984), Vol. 21, p. 11.
[30]A. Frova and A. Selloni, in *Tetrahedrally Bonded Amorphous Semiconductors,* edited by D. Adler and H. Fritzsche (Plenum, New York, 1985), p. 271.
[31]M. Vergnat, N. Maloufi, J. G. Geny, M. Piecuch, G. Marchal, and M. Gerl, in *Poly-micro-crystalline and Amorphous Semiconductors,* edited by P. Pinard and S. Kalbitzer (Editions de Physique, Paris, 1984), p. 707.
[32]S. H. Wemple and M. Didomenico, Phys. Rev. B **3**, 1338, (1971).
[33]S. H. Wemple, Phys. Rev. B **7**, 3767 (1973).
[34]S. H. Wemple, J. Chem. Phys. **67**, 2151 (1977).
[35]J. A. Van Vechten, Phys. Rev. **182**, 891 (1969).
[36]J. C. Phillips, Rev. Mod. Phys. **42**, 317 (1970).
[37]D. R. Penn, Phys. Rev. **128**, 2093 (1962).
[38]M. Cardona, in *Atomic Structure and Properties of Solids,* Proceedings of the International School of Physics "Enrico Fermi" Course 52, Varenna, 1971, edited by E. Burstein (Academic, New York, 1972), p. 514.
[39]R. J. Temkin, G. A. N. Connell, and W. Paul, Solid State Commun. **11**, 1591 (1972).
[40]N. M. Amer and W. B. Jackson, in *Semiconductors and Semimetals,* edited by J. I. Pankove (Academic, Orlando, 1984), Vol. 21, Pt. B, p. 83.

[41]N. Maloufi, A. Audouard, M. Piecuch, and G. Marchal, Phys. Rev. Lett. **56**, 2307 (1986).
[42]M. Mui and F. W. Smith, Phys. Rev. B **35**, 8080 (1987).
[43]H. R. Philipp, J. Phys. Chem. Solids **32**, 1935 (1971); J. Electrochem. Soc. **120**, 295 (1973).
[44]D. E. Aspnes and J. B. Theeten, J. Appl. Phys. **50**,4928 (1979).
[45]D. E. Polk, J. Non-Cryst. Solids **5**, 365 (1971); P. Steinhardt, R. Alben, and D. Weaire, *ibid.* **15**, 199 (1974).
[46]G. A. N. Connell and R. J. Temkin, Phys. Rev. B **9**, 5323 (1974).
[47]J. Dixmier, A. Gheorghiu and M. L. Theye, J. Phys. C **17**, 2271 (1984).
[48]D. A. G. Bruggemann, Ann. Phys. (Leipzig) **24**, 636 (1935).
[49]R. Mosseri and J. Dixmier, J. Phys. (Paris) Lett. **41**, L5 (1980).
[50]C. Senemaud and I. Ardelean (unpublished).